OPEN ACCESS

Surface- and edge-states in ultrathin Bi–Sb films

New Journal of Physics
The open-access journal for physics

Surface- and edge-states in ultrathin Bi–Sb films

G Bihlmayer[1,5], Yu M Koroteev[2,3], E V Chulkov[2,4] and S Blügel[1]

[1] Institut für Festkörperforschung and Institute for Advanced Simulation, Forschungszentrum Jülich, D-52425 Jülich, Germany
[2] Donostia International Physics Center (DIPC), 20018 San Sebastiàn/Donostia, Spain
[3] Institute of Strength Physics and Materials Science, RAS, 634021 Tomsk, Russia
[4] Departamento de Física de Materiales, UPV/EHU, Apartado 1072, 20080 SanSebastiàn/Donostia, Spain
E-mail: g.bihlmayer@fz-juelich.de

New Journal of Physics **12** (2010) 065006 (13pp)
Received 30 September 2009
Published 17 June 2010
Online at http://www.njp.org/
doi:10.1088/1367-2630/12/6/065006

Abstract. Employing first-principles calculations, we studied the electronic structure of ultrathin Bi–Sb films, focusing on the appearance of surface or edge states that are topologically protected. Our calculations show that in ordered structures the Bi–Sb bonds are quite strong, forming well-defined double layers that contain both elements. We find surface states appearing on the (111) surface of a thin film of layerwise ordered Bi–Sb compound, while thin films in (110) orientation are insulating. In the gap of this insulator, edge states can be found in a (110)-oriented ribbon in the A17 (black phosphorus) structure. While these states are strongly spin polarized, their topological properties are found to be trivial. In all structures, we investigate the influence of spin–orbit coupling and analyze spin polarization of the states at the boundaries of the material.

[5] Author to whom any correspondence should be addressed.

Contents

1. Introduction

Electronic states at the boundary of a material can exhibit exotic properties: for example, edge states on insulators in high magnetic fields can carry dissipationless currents, a phenomenon known as the quantum-Hall effect. Without external magnetic fields, spin–orbit coupling (SOC) effects (Rashba effect) can lead to spin accumulation or spin separation (spin Hall effect) in a non-magnetic material. Recently, a new class of material has been predicted that can support dissipationless spin currents: the topological insulators. The existence of this material class has been predicted theoretically for thin films [1, 2] and interfaces of HgTe-based heterostructures [3]. For the latter material, experimental evidence for this new state of matter has been found just 2 years ago by conductivity measurements [4]. In contrast to these structures, surfaces offer the possibility to gain a direct view of those electrons that show this so-called quantum spin-Hall effect (QSHE). Spin- and angle-resolved photoemission and bandstructure calculations offer tools to extract the signature of this effect directly. Therefore, several groups started a search for surface states that show the required electronic properties.

On the surfaces or edges of insulators, states can appear in the (bulk) bandgap that make the boundary of the material conductive. A hallmark of topological insulators is the Fermi contour that results from these states: if the time-reversal invariant midpoints (TRIMs; i.e. the $\overline{\Gamma}$-point and all points in the Brillouin zone that are exactly in between two $\overline{\Gamma}$-points) are encircled by the Fermi contour an odd number of times, the state is topologically nontrivial; if an even number of contours encircle the TRIMs, it is trivial [5]. Whether a material is topologically trivial or not is a bulk property and can be calculated from the so-called time-reversal polarization by a Berry-phase formalism, in some analogy to the calculation of the charge polarization [6]. Unfortunately, these calculations are not always easy and not many materials have been characterized in this way.

Both on the experimental [7, 8] and the theoretical side [9, 10], the surface of $Bi_{1-x}Sb_x$ has attracted considerable interest. Already in the late 1960s, evidence was found that in a concentration range around $x = 0.07$ this alloy has semiconducting properties, while the parent compounds are semimetals [11]. The energy gap is quite small, in the range of 10 meV, and depends on a subtle balance of the shift of the band edges with the concentration, which makes reliable theoretical modeling difficult [9] and slight controversies between theory and experiment remain. Nevertheless, the existence of topologically protected surface states on the

(111) surface is quite firmly established [7]–[10]. This shows that the addition of Sb changes the character of the topologically trivial Bi.

This paper is concerned with the question: How far can these insights from the alloy surface be carried over in the nanoscale regime, e.g. ultrathin films or nanoribbons made of Bi and Sb? In this regime, several phenomena have to be considered that can profoundly change the properties of this alloy: structural effects such as surface segregation of one of the constituents, relaxations or reconstructions, ordering phenomena as well as electronic effects that can result from the confinement of the wavefunctions in nanostructures. For example, in ultrathin Bi films, grown on Si(111), a transition from the A7 structure of bulk Bi to the A17 structure was found below a certain film thickness [12]. The influence of this transition on the electronic structure is dramatic [13]. Also for thicker Bi films, clear consequences of the confinement of the electronic states were seen [14] and have also been discussed recently for topologically nontrivial materials [15].

We investigate systematically possible $Bi_{0.5}Sb_{0.5}$ alloys, first as bulk phases, comparing different structures energetically and from the electronic structure point of view. Using the most stable structure, we construct models of ultrathin films, both in (111) and in (110) orientation, and investigate the surface electronic properties. Finally, we cut out ribbons from the ultrathin film in (110) orientation to examine the possible formation of edge states on these ribbons. Surprisingly, no direct (by calculation of the topological invariants for inversion symmetric structure) or indirect (by inspection of the surface or edge states) evidence for topologically protected states was found in the investigated structures. This indicates that the properties of BiSb nanostructures can depend very sensitively on the actual atomic arrangement and cannot be straightforwardly inferred from the behavior of the (disordered) bulk alloy.

2. Method

For our calculations, we employed density functional theory in the local density approximation [16]. We used the full-potential linearized augmented planewave (FLAPW) method [17] as implemented in the FLEUR code [18]. In all calculations, scalar relativistic corrections were taken into account in the muffin-tin spheres; SOC was included in the self-consistent calculations [19]. In the calculations of the low-dimensional systems, films and ribbons were embedded in semi-infinite vacuum. Monkhorst–Pack k-point sets [20] up to a size of $9 \times 9 \times 9$ (or equivalent in lower dimensions) were used. The muffin-tin radii, R_{mt}, were chosen to be 2.5 a.u. and the size of the LAPW basis was determined by the criterion $K_{\max} R_{\mathrm{mt}} = 9$. The structures were allowed to relax; in these calculations SOC was not included. For the determination of the electronic structure, SOC was included unless stated otherwise.

3. Results

3.1. Bulk material

In bulk Bi and Sb, the nearest-neighbor bonds define double layers with hexagonal symmetry, which might be considered as two hexagonally closed packed lattices or a corrugated honeycomb lattice. In the rhombohedral unit cell, these layers are perpendicular to the (111) direction. We used these (111) layers as building blocks to create Bi–Sb bulk crystals ordering them in different stacking sequences (cf insets in figure 1). Although the Bi–Sb system is

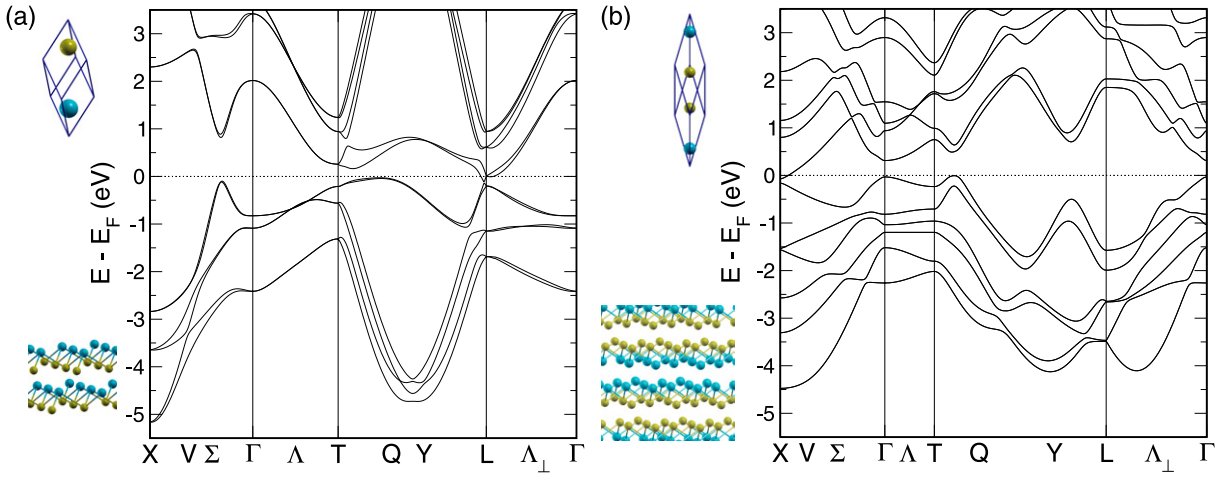

Figure 1. Bulk bandstructures of ordered BiSb alloys. (a) Bandstructure of an alloy built up by alternating Bi and Sb (111) sheets that form Bi–Sb bilayers as indicated in the figures on the left. (b) Bandstructure of an alloy formed from Bi–Sb (111) bilayers, but now with a stacking sequence Bi–Sb–Sb–Bi as indicated by the insets. The notation of the high-symmetry points and lines follows Golin [21]. The structures shown in the insets were produced with the program described in [22].

normally described as an alloy, we think that these structures are not unreasonable: compounds of Bi or Sb with group (VI) metals like Se order in a similar geometry with building blocks in a stacking sequence (Se–Bi–Se–Bi–Se) that is repeated in the (111)-direction to form a Bi_2Se_3 crystal [10].

3.1.1. BiSb. The simplest possible choice is then to alternate single hexagonally closed packed Sb and Bi layers in a two-atom unit cell. In our calculations, we optimized the lattice constant and relaxed the atomic positions to find an optimal geometry. An excellent review of the structure of Bi and its surfaces can be found in [23].

From experimental data it can be concluded that the variations of the rhombohedral angle in these alloys are small [24]. Therefore, we kept the angle fixed at the value for pure Bi (57.35°). The lattice constant was found to be in between the Bi and Sb value, 2.3% smaller than what is found for pure Bi (4.68 Å). As compared to this element, the internal parameter, z, was found to be 1% increased, a tendency that was also found experimentally [24], despite the fact that Sb has a slightly smaller z than Bi [25]. In terms of (111) interlayer distances, these values result in a short- and long-interlayer spacing of 1.60 and 2.20 Å, respectively. This means that Bi–Sb bilayers are formed where each nearest-neighbor bond connects a Bi to an Sb atom with a bonding distance of 3.10 Å, while next-nearest-neighbor Bi–Sb bonds have a length of 3.45 Å.

An investigation of the electronic structure (figure 1(a)) shows clear similarities to the band structures of the parent elements [26]. Since the atomic structure of the compound does not possess inversion symmetry, the number of bands is doubled due to SOC. A remarkable feature can be seen near the L-point, where two bands seem to cross from the valence to the conduction band (actually a tiny gap of 2 meV is found in the calculation). Note that it is exactly at the

L-point where the band structures of Bi and Sb differ: the parity (symmetry with respect to space inversion) of the states that form the upper and lower edges of the gap in Sb is reversed as compared to Bi. This exchange of bands is a consequence of the increased SOC in Bi, as can be seen from calculations, where the SOC strength is artificially decreased from the Bi to the Sb value (see e.g. [11]; we performed a similar calculation that showed qualitatively the same behavior). It is this little detail that leads in Bi to a topologically trivial and in Sb to a nontrivial bandstructure and to severe consequences for the surface states in both materials. Since this layered BiSb alloy does not possess a center of inversion, it is not possible to determine the topological invariants of this material from the symmetry of the wavefunctions at the TRIMs [5] and elaborate calculations would be necessary. But a slight modification of the structure leads to a centrosymmetric system, as will be shown below.

3.1.2. Bi_2Sb_2. Since the Bi and Sb bulk crystals consist, as mentioned above, of double layers, the next natural choice was to consider the stacking Bi–Bi–Sb–Sb–$\cdots$ along the (111)-direction (see figure 1(b)). The nearest-neighbor bonds, however, were not formed by Bi–Bi or Sb–Sb pairs, but rather in between the two elements. The Bi–Sb (3.06 Å) bond is more than 11% shorter than the bond between the Sb atoms, or 14% as compared to the Bi–Bi bond. This means that again Bi–Sb bilayers are formed, but now separated by Bi–Bi and Sb–Sb interfaces. The equilibrium volume is just 1% smaller than pure Bi. Energetically, this stacking sequence is about 30 meV atom^{-1} more unfavorable than the Bi–Sb–Bi–Sb–$\cdots$ stacking discussed in the last section, but at larger volumes it can become the ground state.

From the band structure (figure 1(b)) we can see that also this system is of semi-metallic character, but in contrast to the Bi–Sb–Bi–Sb–$\cdots$ stacking, no bands seem to cross from the conduction to the valence band. Since the structure possesses inversion symmetry, each band is doubly degenerate. Inversion symmetry and the fact that there is a local gap throughout the Brillouin zone allows us to determine also the topological invariants of this material, which are found to equal those of Bi, i.e. (0; 000). This is surprising, as in a disordered alloy, the addition of 7% of Sb to Bi seems to be enough to change the topological character to a nontrivial one, but might be attributed to the fact that we study ordered structures here. Even though this material is topologically trivial, we will see that it shows some interesting properties as a thin film.

3.2. (111) films

The natural cleaving plane in Bi and Sb is the (111) plane. Ultrathin Bi films have been realized on an Si(111) surface [12] and using the same techniques it might also be possible to grow Bi–Sb films in a certain structure. As the smallest units that can probably be realized, we study four-layer films in three different stackings, which correspond to the bulk structures investigated in the last section. We start with the energetically most stable configuration, that is, in contrast to what could be expected from the bulk phases, the Bi–Sb–Sb–Bi stacking.

3.2.1. Bi–Sb–Sb–Bi. Structurally, this film is very similar to the corresponding bulk material: the interlayer distance of the Sb–Bi bilayer was found to be 1.61 Å, while the inner Sb–Sb plane separation was 2.36 Å (in the bulk, these values are 1.58 and 2.25 Å, respectively).

An investigation of the electronic structure including SOC (red lines in figure 2, left) shows an electron pocket at the $\overline{\Gamma}$-point with a single, doubly degenerate state forming a circle at the Fermi surface around the zone center. Comparison to the bulk bandstructure (e.g. along

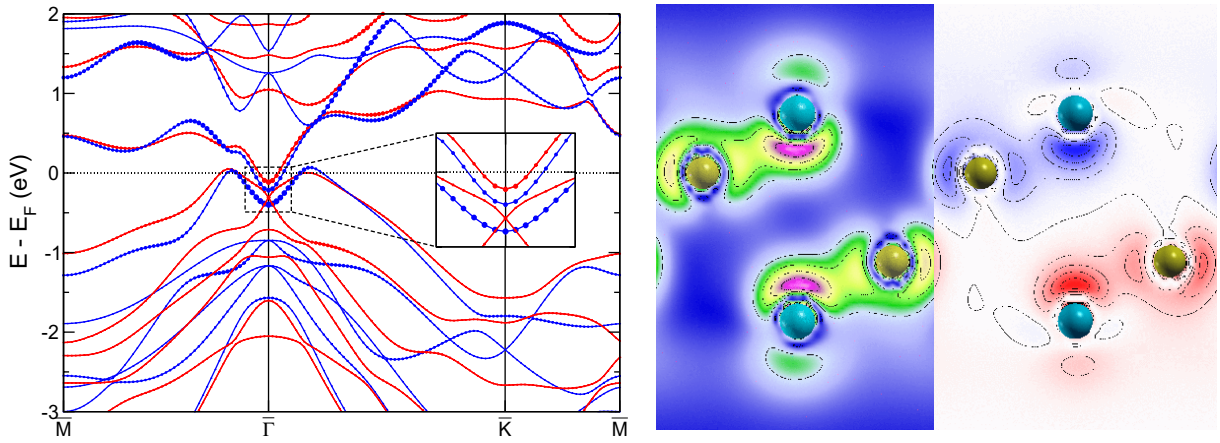

Figure 2. Left: bandstructure of a four-layer film in (111) orientation with the stacking sequence Bi–Sb–Sb–Bi. Blue and red lines indicate calculations without and with SOC, respectively. The size of the symbols corresponds to the weight of the state in the vacuum. The inset shows a magnification of the bandstructure around the $\overline{\Gamma}$-point. In the middle and right panels, the charge and spin density of the state at 0.08 $\overline{\Gamma M}$ at the Fermi level are shown, respectively. The isolines in both plots indicate density steps of 3 me^{-} $(\mathrm{a.u.})^{-3}$; in the spin-density plot, red and blue indicate positive and negative values, respectively.

the line Γ–T that projects on the $\overline{\Gamma}$-point) shows that in this region bands are formed outside the projected bulk bandstructure. Indeed, a similar state was found for a pure Bi film and its evolution to the surface state in Bi(111) was demonstrated in [27].

Closer inspection of figure 2 shows that there are no states crossing from the valence to the conduction band region. Although in these ultrathin films quantization effects can lead to splittings of topologically protected states that cross from the valence to the conduction band [15], which can result in a bandstructure like the present one, from the topological properties of the bulk material we can conclude that this is not the case here.

Depending on the exact position of the Fermi level—which might be varied by doping, as demonstrated for another Bi compound [28]—additional Fermi surface features can arise from the hole pockets that can be seen along the $\overline{\Gamma M}$ and $\overline{\Gamma K}$ lines. Since these features can be removed from the Fermi level, we will not discuss them here further.

When we switch off SOC in our calculations (blue lines in figure 2), it is seen that this electron pocket is hardly changed, while other bands show clear spin–orbit-induced modifications. From the weight of the states in the vacuum region, we can also see that the states forming this pocket are directed to some extent towards the vacuum, i.e. they have a p_z component. From the charge density plot (middle panel of figure 2) they can be characterized as (Sb-p_x, Bi-p_z) hybrids. Similar bonds are found near the zone center of Bi(111) films [27]. Since we have a symmetric film, two degenerate bonds are found in both bilayers. When we look at the spin density (with the spin-quantization axis chosen perpendicular to the surface normal and to the propagation direction as defined by the $\mathbf{k}_{\parallel}$-vector), we find that in each bilayer these states are almost completely spin polarized with opposite orientations in the upper and lower bilayers (right panel of figure 2).

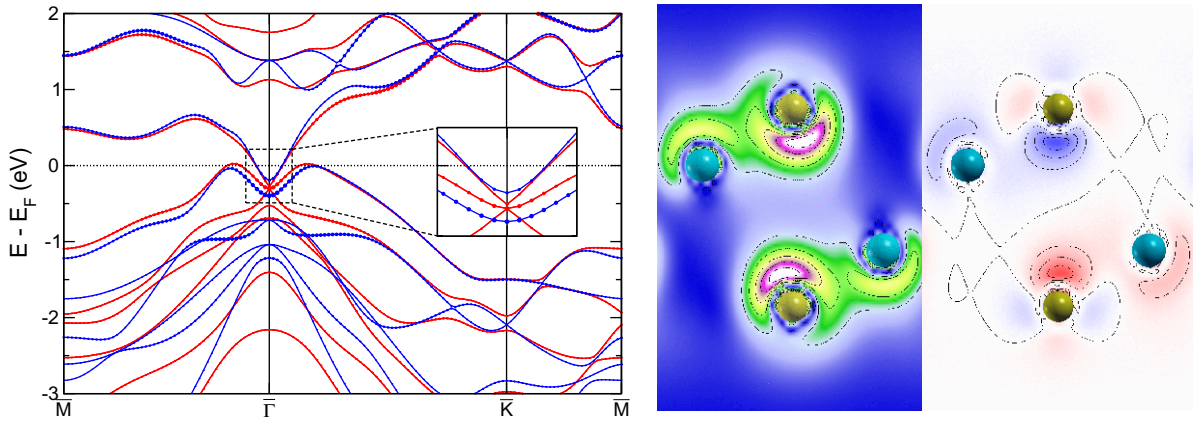

Figure 3. Left: band structure of a four-layer film in (111) orientation with the stacking sequence Sb–Bi–Bi–Sb, drawn in the same manner as figure 2. Right: charge and spin-density plots of the state at 0.08 $\overline{\Gamma M}$ near the Fermi level. All parameters were chosen as in figure 2.

Although globally the degenerate pair of bands that form the Fermi surface is non-polarized, locally a strong spin polarization is obtained. Therefore, each surface of this ultrathin film shows already interesting spin-dependent transport properties and can be easily decoupled from the other surface by breaking the inversion symmetry, e.g. when the film is deposited on a substrate. For example, spin-selective quasi-particle interference as it was found for clean Bi(110) [29] and recently also for a BiSb alloy [30] should show up here as well.

3.2.2. Sb–Bi–Bi–Sb. Another thin film can be obtained from the Bi–Bi–Sb–Sb–$\cdots$ stacked bulk material when the surface is opened between the Sb layers. Upon relaxing this structure, the interlayer distance of the Sb–Bi bilayer was found to be 1.58 Å, while the inner Bi–Bi plane separation was 2.38 Å. As compared to the Bi–Sb–Sb–Bi film, this structure turns out to be 72 meV atom^{-1} less stable, i.e. there is a clear preference for Bi at the surface.

The electronic structure of this film is shown in figure 3. If we compare the bandstructure obtained without SOC (blue lines) to that of the Bi–Sb–Sb–Bi film (figure 2), we note the close similarity between the two cases. This is not surprising, since we know that both Bi and Sb are chemically very similar and the major difference consists in the SOC. If SOC is neglected, the differences become rather small, but if it is included they can be seen clearly. These differences are then also enhanced by the presence of surfaces, which break the inversion symmetry locally. To some extent this influences even the energetics, e.g. the energy difference between the Sb–Bi–Bi–Sb and the Bi–Sb–Sb–Bi film decreases from 72 to 50 meV when SOC is not taken into account. Since these energy differences are of considerable size, it is *a priori* not clear whether the surface of a disordered BiSb alloy will maintain its disordered character or segregation effects (chemically and SOC-induced) will occur.

Comparing the electronic structure with SOC included (red lines in figures 2 and 3), we can observe gap openings occurring with very different size in both cases: for example, the bottom of the conduction band at the $\overline{\text{K}}$-point is formed by states with surface-state character; therefore they are mainly Bi-derived in the Bi–Sb–Sb–Bi film and Sb-derived in the Sb–Bi–Bi–Sb case; accordingly the splitting is much stronger in the former case than in the latter. Similar effects

can also be seen around the $\overline{\Gamma}$-point (insets of the figures), although the Fermi contour itself is hardly changed. Also, if we look at the spin densities of these states, the properties are found to be rather similar, with a slightly reduced local spin polarization at the Sb-terminated surface. From the charge density plots, we note a visible change of the orbital character of the inner layers and a tilting of the p_z orbital in the outer layer as compared to the Bi–Sb–Sb–Bi film.

3.2.3. Bi–Si–Bi–Sb. As a third possible structure we chose a four-layer film created from the Bi–Sb–Bi–Sb–$\cdots$ stacked bulk. Structurally, this film is in between the two previous ones, showing interlayer distances of 1.60 and 2.37 Å for the outer and inner interlayer spacing, respectively. As compared to the Bi–Sb–Sb–Bi film, this structure turns out to be 23 meV atom^{-1} less stable, although from the investigations of the bulk structures one could expect this ordering to be most stable. On the other hand, we know from the last section that the formation of an Sb-terminated surface is energetically disfavored by 36 meV atom^{-1} for one surface as compared to a Bi-terminated one. With increasing film thickness, we can expect that this energy is quickly compensated and that Bi–Sb–Bi–Sb–$\cdots$ stacked films will get energetically favorable.

When we discuss the electronic structure, we have to keep in mind that this film does not possess inversion symmetry, so the number of bands is doubled with respect to the cases discussed above. This leads to the fact that each individual band is now spin polarized, as can be seen from the inset of figure 4. In a small region around the zone center and the Fermi level, we observe in total six bands, one pair seemingly crossing from the conduction to the valence band, another one showing the opposite dispersion, and a rather flat one in between. All bands meet in a small energy interval, around −0.32 eV. A closer look reveals that the two strongly dispersive bands do not cross, but split by 60 meV. Thus, the situation at the $\overline{\Gamma}$-point is similar to what is seen in figure 3, where a 30 meV splitting was found. Moving away from the zone center, for all bands a $\mathbf{k}_{\|}$-dependent splitting is found that separates the bands according to spin and their localization on one particular surface. As an example, we show again states with an energy at the Fermi level with the smallest possible $\mathbf{k}_{\|}$-vector on the right of figure 4.

3.3. (110) films

For Bi films below a certain thickness, a structural transition to the A17 structure has been observed [12] and the films display the pseudocubic (110) surface.

Two possible structures of these thin films are displayed in figure 5, one corresponding to a bulk structure with an alternating stacking of Bi and Sb (111) layers, and one made of Bi and Sb bilayers, as discussed above. It can be seen that both structures relax in a unique pattern, resembling the ultrathin Bi films reported in [12]. We see that most of the bonds are considerably shorter than in the bulk, where a Bi–Sb bond length of 3.06–3.10 Å was found (section 3.1). Furthermore, we observe that the bonds connecting the upper and the lower surface are shorter than the bonds in the surface layers. Energetically, it turns out that the energy difference of both structures is just 3 meV atom^{-1}, in favor of the arrangement shown in the upper panel of figure 5. As compared to the (111) oriented films, these structures are about 30 meV atom^{-1} less stable, in contrast to the findings in the pure Bi films, where (110) oriented films in the A17 structure were found to be energetically favorable for small film thicknesses.

To analyze the electronic structure of these films, we show on the left of figure 6 the band structure of the Bi–Sb film with the lowest total energy, i.e. the structure as shown in the top panel of figure 5. A bandgap of more than 0.5 eV around the Fermi level can be observed, which

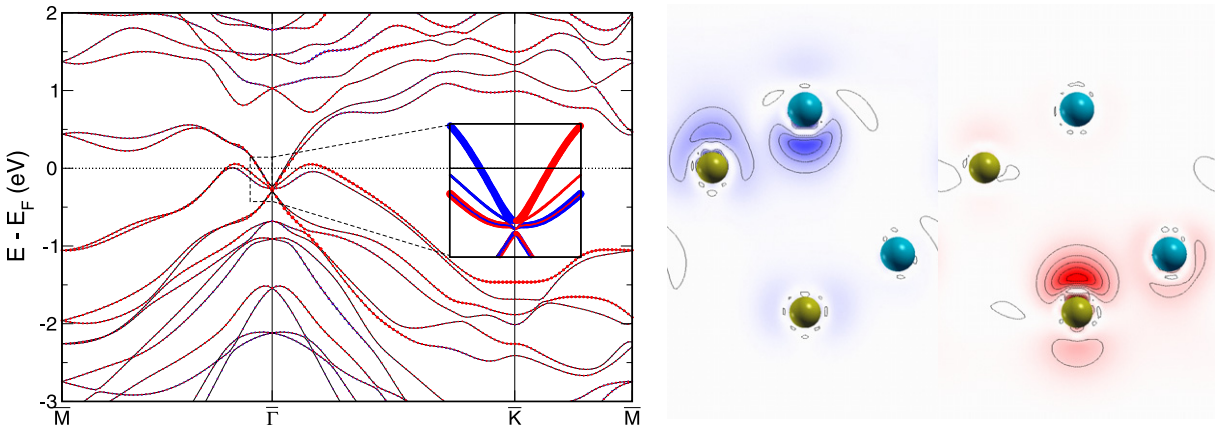

Figure 4. Left: band structure of a four-layer film in (111) orientation with the stacking sequence Bi–Sb–Bi–Sb. SOC was included in the calculation. Inset: band structure in the $\overline{\mathrm{M}}$–$\overline{\Gamma}$–$\overline{\mathrm{M}}$ direction in a small region around the zone center. The color indicates the spin-orientation and the size of the symbols the spin-polarization in the topmost Bi layer with respect to a direction perpendicular to the surface normal and the $\mathbf{k}_{\parallel}$-vector. Right: spin density plots of the bands at 0.08 $\overline{\Gamma\mathrm{M}}$ near the Fermi level. The isolines in both plots indicate spin-density steps of $3\,\mathrm{me}^{-}\,(\mathrm{a.u.})^{-3}$. Red and blue indicate positive and negative values, respectively.

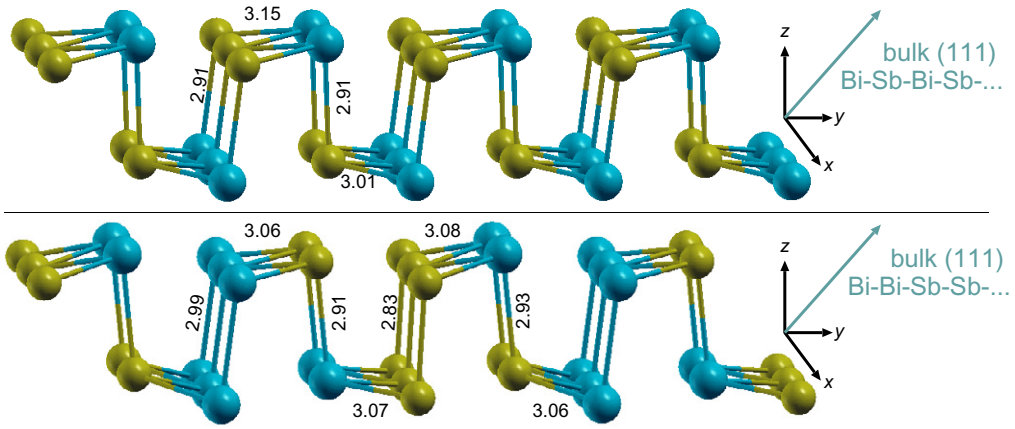

Figure 5. Structure of ultrathin Bi–Sb films displaying a pseudocubic (110) surface. The top panel shows a film with an arrangement of atoms corresponding to Bi–Sb–Bi–Sb–· · · (111) planes in the bulk, whereas in the lower panel the structure is Bi–Bi–Sb–Sb–· · · like. The numbers indicate the bond length in ångströms. The coordinate systems show the surface normal in the z-direction, the bulk (111) direction and the ordering of the (111) planes in the bulk are indicated on the right.

renders this film a useful starting point for the investigation of edge states that could form inside the gap. For comparison, we calculated the band structure for the (110) film cut out from the Bi–Bi–Sb–Sb–· · · stacked bulk (lower panel of figure 5) and we found that in this case a similar bandstructure with a gap of comparable size is obtained (not shown).

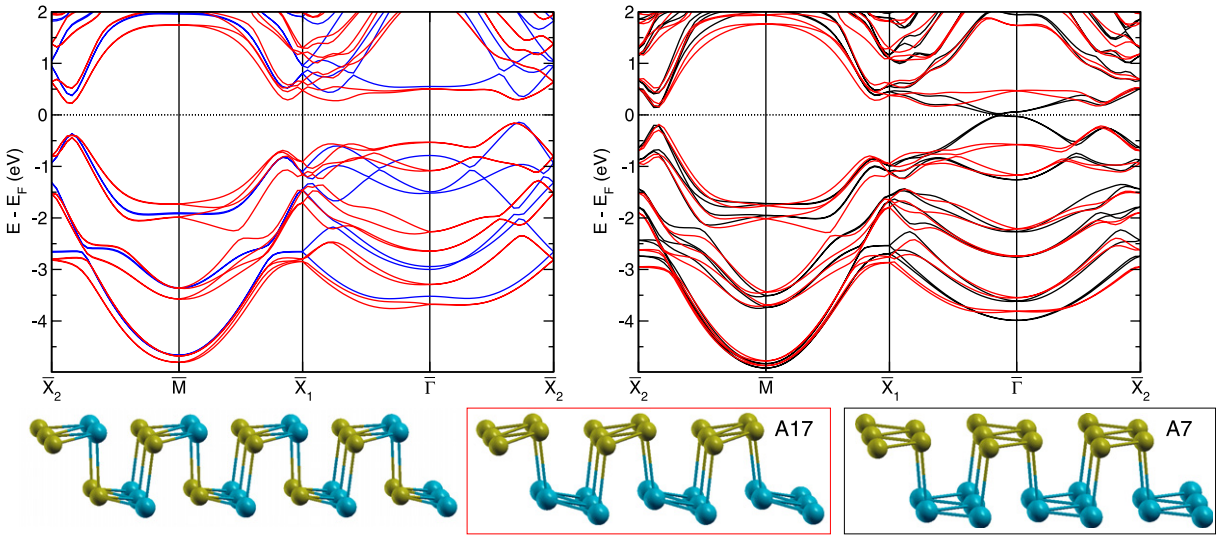

Figure 6. Left: band structure of a Bi–Sb film in (110) orientation as shown in the bottom left figure. The calculation with SOC included is shown with red lines and that without SOC is shown in blue. Right: band structure (including SOC) of a Bi–Sb film with atoms ordered as shown in the lower middle and right figures. The black lines correspond to the unbuckled A7 structure and the red lines to the buckled A17 structure. Without SOC the bandstructures resemble closely the calculation on the left (blue lines), with the exception that in the A7 structure the bandgap at $\overline{\Gamma}$ is somewhat reduced.

Nevertheless, also in the case of (110) oriented thin films, the influence of SOC on the bandstructure can depend sensitively on the arrangement of the atoms. This can be seen on the right of figure 6, where we show the bandstructure of a film that consists of a pure Bi bilayer on one surface and a pure Sb bilayer on the other one (see inset). This corresponds to a rather complicated Bi/Sb ordering in the bulk, but is a situation that could be produced by surface segregation, e.g. in thicker films. This film is about 20 meV atom^{-1} less stable as the stacking shown in the bottom left of figure 6. As long as the buckled black-phosphorus structure (A17) is maintained, the bandstructure shows a gap, a feature that was also found for ultrathin Bi films [13]. But when we transform the structure to the rather flat A7 type (lower right image in figure 6), we observe that bands appear in the bandgap crossing from the valence to the conduction band, leading to a semi-metallic structure. This is a pure spin–orbit effect, since the bandstructure calculated without SOC resembles closely the one of the A17 structure, irrespective of the ordering (i.e. left or middle image at the bottom of figure 6).

The comparison between the films in the A7 and A17 structures can be seen as an example of non-protected surface states, which arise in the flat A7 geometry but are removed by the corrugation of the A17 allotrope.

3.4. (110) ribbons

To investigate the possible formation of edge states in (110) oriented BiSb films, we started from the structure shown in the top panel of figure 5 and cut out a 16-atom (about 18 Å) wide ribbon, terminated on one side with an Sb atom and on the other side with a Bi. Since these

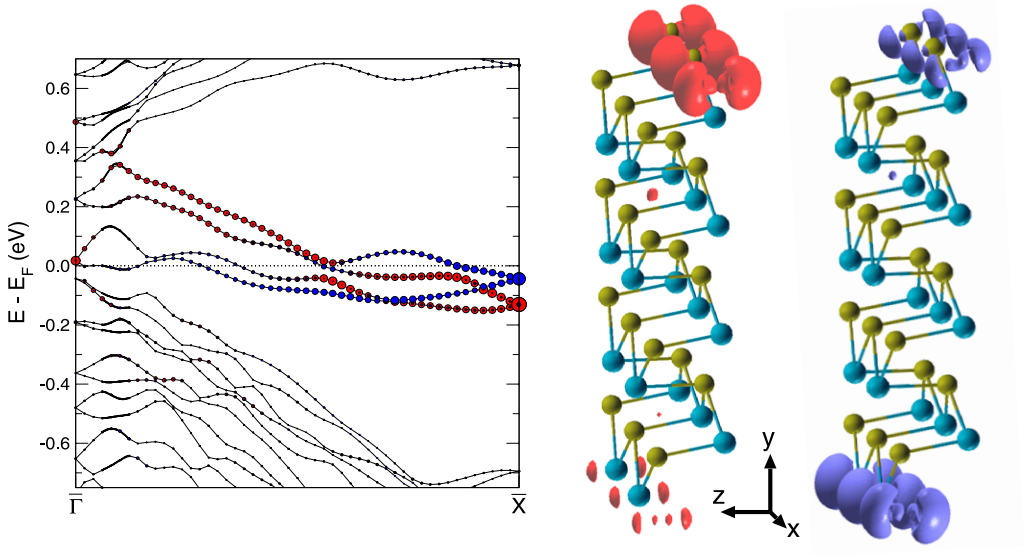

Figure 7. Band structure of a Bi–Sb ribbon (left) and the corresponding structural model (middle and right). The weight of the states at the Sb edge is shown by the size of the red symbols; for the Bi-terminated edge, blue symbols are used. Two spin–orbit split edge states appear in the bandgap; the charge distribution of the states at the $\overline{\mathrm{M}}$-point is shown in the middle and right figures for the Sb and Bi edges, respectively. The coordinate system again shows the surface normal in the z-direction.

atoms have one dangling bond, the formation of edge states is very likely. A similar behavior is found on Bi surfaces where the surface atoms are left with one dangling bond, e.g. the (100) surface, which shows pronounced surface states [31]. Although strong relaxations are found on this surface, no reconstructions remove these surface states [32].

From the bandstructure of the Bi–Sb (110) film (left of figure 6), we expect that the ribbon also shows a bandgap where the local gap at the zone center (on which the $\overline{\Gamma}$ and $\overline{\mathrm{X}}_2$-points of the two-dimensional bandstructure project) is smaller than at the zone edge (projection of the $\overline{\mathrm{M}}$ and $\overline{\mathrm{X}}_1$-points). Inside this gap, we observe the formation of four states, corresponding to two spin-split edge states from either side of the ribbon (figure 7). Near the TRIMs, $\overline{\Gamma}$ and $\overline{\mathrm{M}}$, a Rashba-type splitting (linear in $\mathbf{k}_{\|}$) can be observed. We see that the bands associated with the Bi edge stay near the Fermi level in the whole Brillouin zone, while the states from the Sb edge show more dispersion and almost touch the conduction band near $\overline{\Gamma}$.

Also in this example no evidence for a topologically protected edge state could be found. Therefore, calculations with larger unit cells that allow for dimerization of the edge atoms or other reconstructions are necessary to see whether these states will be stable in a relaxed geometry.

4. Conclusions

We investigated the atomic and electronic structure of ordered $\mathrm{Bi}_{0.5}\mathrm{Sb}_{0.5}$ alloys in different dimensionalities. Structurally, these alloys are characterized by bilayer formation with strong Bi–Sb bonds, while homoatomic bonds are considerably weaker. In all cases we found that

the electronic structure can depend quite sensitively on the actual atomic arrangement, e.g. interchanging of Bi and Sb between the bilayers. Already in the thinnest (111) films interesting Fermi-surface topologies can be found: even though these states might not be topologically protected, spin-dependent scattering on the surfaces can lead to interesting properties for spin-dependent transport. In contrast to the (111) oriented films, the (110) films were found to be insulating with gaps of up to 0.5 eV in most cases. In quasi-one-dimensional structures, small ribbons cut out of these films, we found well-defined edge-states forming in the gap. Even though these ribbons were just 18 Å wide, well-separated states formed on both edges.

Although no evidence for topologically protected states was found, we think that insight into the electronic properties of these nanostructures can help in the understanding of materials that are discussed as topological insulators. Up to now, most insights into this material class are derived from bulk or surface properties. On the nanoscale, a large diversity in the electronic properties can be expected that might be difficult to control, but also offer additional functionality in these alloys. Other aspects, like the influence of disorder and the interaction with a substrate, provide numerous possibilities for future investigations.

Acknowledgments

GB is grateful for the hospitality of the Donostia International Physics Center, where part of this work originated, and the financial support of the Deutsche Forschungsgemeinschaft (grant no. BI823/1-1).

References

[1] Kane C L and Mele E J 2005 *Phys. Rev. Lett.* **95** 146802
[2] Murakami S 2006 *Phys. Rev. Lett.* **97** 236805
[3] Bernevig B A, Hughes T L and Zhang S-C 2006 *Science* **314** 1757
[4] König M, Wiedmann S, Brüne C, Roth A, Buhmann H, Molenkamp L W, Qi X-L and Zhang S-C 2007 *Science* **318** 766
[5] Fu L and Kane C L 2007 *Phys. Rev.* B **76** 045302
[6] Fu L and Kane C L 2006 *Phys. Rev.* B **74** 195312
[7] Hsieh D, Qian D, Wray L, Xia Y, Hor Y S, Hasan R J and Cava M Z 2008 *Nature* **452** 970
[8] Hsieh D *et al* 2009 *Science* **323** 919
[9] Teo J C Y, Fu L and Kane C L 2008 *Phys. Rev.* B **78** 045426
[10] Zhang H, Liu C-X, Qi X-L, Fang Z and Zhang S-C 2009 *Nat. Phys.* **5** 438
[11] Tichovolsky E J and Mavroides J G 1969 *Solid State Commun.* **7** 927
[12] Nagao T, Sadowski J T, Saito M, Yaginuma S, Fujikawa Y, Kogure T, Ohno T, Hasegawa Y, Hasegawa S and Sakurai T 2004 *Phys. Rev. Lett.* **93** 105501
[13] Yaginuma S, Nagaoka K, Nagao T, Bihlmayer G, Koroteev Yu M, Chulkov E V and Nakayama T 2008 *J. Phys. Soc. Japan* **77** 014701
[14] Hirahara T *et al* 2008 *New J. Phys.* **10** 083038
[15] Lu H-Z, Shan W-Y, Yao W, Niu Q and Shen S-Q 2009 arXiv:0908.3120
[16] Moruzzi V L, Janak J F and Williams A R 1978 *Calculated Electronic Properties of Metals* (New York: Pergamon)
[17] Wimmer E, Krakauer H, Weinert M and Freeman A J 1981 *Phys. Rev.* B **24** 864
[18] http://www.flapw.de
[19] Li C, Freeman A J, Jansen H J F and Fu C L 1990 *Phys. Rev.* B **42** 5433

[20] Monkhorst H J and Pack J D 1976 *Phys. Rev.* B **13** 5188
[21] Golin S 1968 *Phys. Rev.* **166** 643
[22] Kokalj A 2003 *Comp. Mater. Sci.* **28** 155
[23] Hofmann Ph 2006 *Prog. Surf. Sci.* **81** 191
[24] Cucka P and Barrett C S 1962 *Acta Cryst.* **15** 865
[25] Barrett C S, Cucka P and Haefner K 1963 *Acta Cryst.* **16** 451
[26] Gonze X, Michenaud J-P and Vigneron J-P 1990 *Phys. Rev.* B **41** 11827
[27] Koroteev Yu M, Bihlmayer G, Chulkov E V and Blügel S 2008 *Phys. Rev.* B **77** 045428
[28] Hsieh D *et al* 2009 *Nature* **460** 1101
[29] Pascual J I *et al* 2004 *Phys. Rev. Lett.* **93** 196802
[30] Roushan P, Seo J, Parker C V, Hor Y S, Hsieh D, Qian D, Richardella A, Hasan M Z, Cava R J and Yazdani A 2009 *Nature* **460** 1106
[31] Hofmann Ph, Gayone J E, Bihlmayer G, Koroteev Yu M and Chulkov E V 2005 *Phys. Rev.* B **71** 195413
[32] Sun J, Wang J, Wells J, Koroteev Yu M, Bihlmayer G, Chulkov E V, Hofmann Ph and Pohl K *New J. Phys.* submitted